Journal of Medicinal Chemistry

ARTICLE

pubs.acs.org/jmc

Discovery of a Potent and Efficacious Peptide Derivative for δ/μ Opioid Agonist/Neurokinin 1 Antagonist Activity with a 2′,6′-Dimethyl-L-Tyrosine: In vitro, In vivo, and NMR-Based Structural Studies

Takashi Yamamoto,[†,§] Padma Nair,[†] Tally M. Largent-Milnes,[‡] Neil E. Jacobsen,[†] Peg Davis,[‡] Shou-Wu Ma,[‡] Henry I. Yamamura,[‡] Todd W. Vanderah,[‡] Frank Porreca,[‡] Josephine Lai,[‡] and Victor J. Hruby*[,†]

[†]Department of Chemistry and Biochemistry, University of Arizona, 1306 East University Boulevard, Tucson, Arizona 85721, United States

[‡]Department of Pharmacology, University of Arizona, 1501 North Campbell Avenue, Tucson, Arizona 85724, United States

Supporting Information

ABSTRACT: Multivalent ligands with δ/μ opioid agonist and NK1 antagonist activities have shown promising analgesic potency without detectable sign of toxicities, including motor skill impairment and opioid-induced tolerance. To improve their biological activities and metabolic stability, structural optimization was performed on our peptide-derived lead compounds by introducing 2′,6′-dimethyl-L-tyrosine (Dmt) instead of Tyr at the first position. The compound 7 (Dmt-D-Ala-Gly-Phe-Met-Pro-Leu-Trp-NH-[3′,5′-$(CF_3)_2$-Bzl]) showed improved multivalent bioactivities compared to those of the lead compounds, had more than 6 h half-life in rat plasma, and had significant antinociceptive efficacy in vivo. The NMR structural analysis suggested that Dmt[1] incorporation in compound 7 induces the structured conformation in the opioid pharmacophore (N-terminus) and simultaneously shifts the orientation of the NK1 pharmacophore (C-terminus), consistent with its affinities and activities at both opioid and NK1 receptors. These results indicate that compound 7 is a valuable research tool to seek a novel analgesic drug.

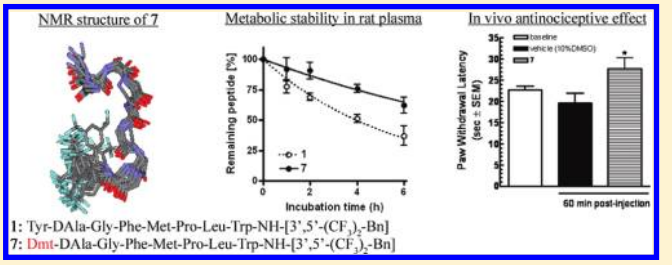

INTRODUCTION

The treatment of pain, especially prolonged and neuropathic pain, is a major challenge and millions of people suffer from such pain every day. Opioids remain the mainstay for the treatment of these pain states. However, sustained opioid treatment is associated with serious unwanted effects including somnolence and mental clouding, nausea and vomiting, and constipation. Analgesic tolerance to opioid therapy also develops in many patients with continued use. These side effects significantly decrease the patients' quality of life. The mechanisms for these side effects are still largely unclear. Prolonged pain states lead to neuroplastic changes in both ascending and descending pathways in the spinal column in which there is both an increased release of neurotransmitters (e.g., substance P) that enhance pain and increased expression of the corresponding receptors for those newly released pain-promoting ligands.[1−3] Current treatment of prolonged pain generally can only modulate pain and cannot counteract against these induced neuroplastic changes. Thus, it is not surprising that current analgesic drugs do not work well in these pathological conditions.

Recently, coadministrations of a δ/μ opioid agonist and a neurokinin 1 (NK1) antagonist have been tested to study the facilitatory role of the substance P-NK1 system in opioid signal transmission. This combination elucidates several important biological effects such as enhanced potency in acute pain models[4] and prevention of opioid-induced tolerance in chronic tests using rats.[5] Another study reported that NK1 knockout mice did not show the rewarding properties of morphine.[6] Thus, the combination of an agonist at the opioid receptors and an antagonist at NK1 receptors may have synergistic effects in the treatment of prolonged pain states that involve enhanced substance P activity. Drug cocktails have limitations as therapeutics because of poor patient compliance, complications in drug metabolism, distribution, and possible drug−drug interactions. We have taken a new approach to combine these two activities in one ligand which should have simple metabolic and pharmacokinetic properties. The desirable activities of our ligand would include potent analgesic affects in both acute pain and in neuropathic pain states without the development of tolerance.[7] Our working drug-design strategy is based on the adjacent and overlapping pharmacophores concept, in which the opioid agonist pharmacophore is incorporated at the N-terminus and the NK1 antagonist pharmacophore locates at the C-terminus of a single peptide derived molecule. The opioid pharmacophore of these chimeric peptides were designed based on the sequence of biphalin and DADLE,[8,9] while the

Received: August 5, 2010
Published: March 02, 2011

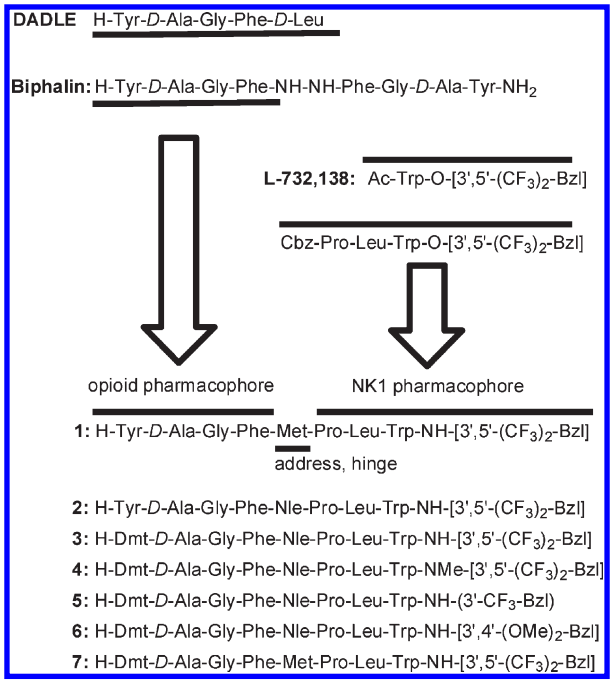

Figure 1. Sequences of multivalent ligands.

structures from 3′,5′-(bistrifluoromethyl)-benzyl ester of *N*-acylated tryptophans were modified with amino acid residues into the NK1 antagonist pharmacophore.[10−12] The important fifth residue works as an address region for both pharmacophores as well as a hinge between them (Figure 1).[9,13−16] It should be emphasized that the designed multivalent chimeric molecules have additional advantages over a cocktail of individual drugs for easy administration, a simple ADME property and no drug−drug interaction. A higher local concentration is also expected than that in the coadministration of two drugs because the expressions of the NK1 and opioid receptors show a significant degree of anatomical overlap in the central nervous system, leading to synergies in potency and efficacy.[17−19] In fact, our previous results showed that the lead bifunctional compounds, TY005 (Tyr^1-D-Ala^2-Gly^3-Phe^4-Met^5-Pro^6-Leu^7-Trp^8-O-[3′,5′-Bzl(CF$_3$)$_2$]) and TY027 (**1**: Tyr^1-D-Ala^2-Gly^3-Phe^4-Met^5-Pro^6-Leu^7-Trp^8-[NH-3′,5′-Bzl(CF$_3$)$_2$]), have been shown to reverse neuropathic pain in a rodent model with blood−brain barrier permeability, no sign of opioid-induce tolerance, and no development of reward liability, validating our hypothesis that a single compound possessing opioid agonist/NK1 antagonist activities is effective against neuropathic pain.[7,20−23] The structural differences between the two lead compounds were in their C-terminus, which was crucial for both opioid and NK1 activities.[9] The C-terminal ester (TY005) has a short half-life in rat plasma (about 1 min), while C-terminal amide (**1**) had a half-life of 4.8 h. The substitution of Met^5 with Nle (**2**) resulted in improved stability (the half-life was more than 6 h) with nearly equipotent activities at both opioid and NK1 receptors compared to **1**.[14]

To perform a lead-to-drug-candidate structural optimization, we sought further improvement in the biological activities and metabolic stability. Extensive studies previously indicated that the substitution of 2′,6′-dimethyl-L-tyrosine (Dmt) for Tyr^1 in opioid peptides produces, in general, a significant increase in opioid receptor affinity,[24−26] and thus this modification could be a critically effective strategy to improve opioid agonist activities in the bifunctional peptides, although the influence of Dmt^1-introduction for the NK1 activity was not known. Thus, an SAR study was initiated by the incorporation of Dmt^1 in compound **2**, followed by modification on the C-terminal and fifth position, to optimize both opioid and NK1 activities. Further elucidation of the biological and conformational effect of Dmt^1-incorporation was performed using the NMR structure based on distance and φ dihedral angle constraint information.

The bifunctional peptide derivatives **3**−**7** were synthesized using procedures previously described.[13,15] The biological activities of **3**−**7** were extensively evaluated on our well-established radioligand binding assays, guanosine 5′-(γ-thio) triphosphate (GTPγS) binding assays, and isolated tissue-based functional assays using guinea pig ileum (GPI) and mouse isolated vas deferens (MVD) tissues.[9,13,15] The metabolic stabilities of compounds were tested by incubation in rat plasma at 37 °C.[14] The in vivo antinociceptive potency of the peptide derivative was confirmed using noninjured rats.[20,22,23]

RESULTS AND DISCUSSION

Biological Activities. The SAR study was initiated by incorporating Dmt at the first position of **2** to yield **3** (Figure 1). Although this modification was made in the opioid-agonist pharmacophore, **3** showed a 10-fold decrease in binding affinity at the human NK1 (hNK1) receptor compared to that of **2**, indicating the influence of the N-terminus (Table 1). This implies that the first residues of the peptide sequences work as an address region for the hNK1 receptor. It should be noted that the Dmt^1-introduction induced relatively smaller shifts in binding affinity for the rat NK1 (rNK1) receptor, as well as in the functional activity using the GPI (Table 2). **3** had improved binding affinity at the μ opioid receptor (MOR) in the low nanomolar range, while the affinity at the δ opioid receptor (DOR) was 10-fold less than that of **2**. This compound has about 9-fold selectivity for the μ-opioid receptors. Compound **4**, which has an *N*-methylated C-terminus, showed high affinities for both the δ- and μ-opioid receptors, implying that the C-terminus modification has a strong influence on the opioid activities (K_i = 0.46 and 1.8 nM, respectively; Table 1). Thus, the two pharmacophores in our bifunctional compounds do not work independently but interact with each other as a single ligand which can enhance binding at both the opioid and NK1 receptors. Consistent with the binding affinities, the functional activities of **4** in conventional isolated-tissue based assays were improved from those of **2** (14 and 110 nM for MVD and GPI assays, respectively; Table 2). However, the binding affinity of **4** for the hNK1 receptor was not as potent as **2** (K_i = 0.21 nM). We next examined the monotrifluoromethyl derivative of **3** (**5**, Figure 1). Compound **5** exhibited decreased NK1 binding affinities (K_i = 1.0 and 140 nM for human and rat NK1 receptors, respectively) and lower functional activity (K_e = 24 nM) compared to those of **3** (Table 1). The affinities of **5** were better at opioid receptors similar to those of **3**. The introduction of electron-dominating methoxy groups at the C-terminus was also tested (**6**, Figure 1). Interestingly, compound **6** had the best opioid affinities among the tested ligands **3**−**7** with subnanomolar K_i values both at the δ- and μ-opioid receptors (0.15 and 0.34 nM, respectively). GTPγS binding assays (Table 3) also demonstrated that **6** had potent opioid activities at both the δ- and μ- opioid receptors (EC_{50} = 0.60 and 0.72 nM, respectively; Table 3). Higher potency for opioid activities also was observed in the isolated tissue bioassays using the MVD and GPI (Table 2), suggesting

Table 1. Binding Affinities of Bifunctional Peptide Derivatives at δ/μ Opioid Receptors and NK1 Receptors

	hDOR[a], [^{3}H]DPDPE[b]		rMOR[a], [^{3}H]DAMGO[c]			hNK1[d], [^{3}H]substance P[e]		rNK1[d], [^{3}H]substance P[f]		
compd	Log IC_{50}[g]	K_i (nM)	Log IC_{50}[g]	K_i (nM)	$K_i(\mu)/K_i(\delta)$	Log IC_{50}[g]	K_i (nM)	Log IC_{50}[g]	K_i (nM)	K_i(hNK1)/K_i(rNK1)
1[h]	−8.84 ± 0.07	0.66	−7.44 ± 0.05	16	24	−10.91 ± 0.10	0.0065	−7.61 ± 0.03	7.3	1100
2[i]	−8.67 ± 0.05	1.0	−7.17 ± 0.07	32	32	−11.57 ± 0.59	0.0028	−7.68 ± 0.03	6.8	2400
3	−7.62 ± 0.10	11	−8.60 ± 0.03	1.2	0.11	−9.78 ± 0.04	0.075	−7.28 ± 0.06	13	170
4	−9.01 ± 0.11	0.46	−8.48 ± 0.1	1.8	3.9	−9.33 ± 0.04	0.21	−7.51 ± 0.08	11	52
5	−8.07 ± 0.06	4.1	−8.82 ± 0.04	0.74	0.18	−8.66 ± 0.04	1.0	−6.41 ± 0.04	140	140
6	−9.50 ± 0.11	0.15	−9.20 ± 0.05	0.34	2.3	−8.70 ± 0.03	0.95	−6.05 ± 0.03	320	340
7	−9.42 ± 0.08	0.18	−8.37 ± 0.15	2.0	11	−10.74 ± 0.04	0.0079	−8.29 ± 0.35	2.3	290
biphalin[j]		2.6		1.4	0.54					
L-732,138						−8.83 ± 0.02	0.73	−6.40 ± 0.03	130	180

[a] Competition analyses were carried out using membrane preparations from transfected HN9.10 cells that constitutively expressed the DOR and MOR, respectively. [b] K_d = 0.45 ± 0.1 nM. [c] K_d = 0.50 ± 0.1 nM. [d] Competition analyses were carried out using membrane preparations from transfected CHO cells that constitutively expressed rat or human NK1 receptors. [e] K_d = 0.16 ± 0.03 nM. [f] K_d = 0.40 ± 0.17 nM. [g] The logIC_{50} ± standard error are expressed as logarithmic values determined from the nonlinear regression analysis of data collected from at least two independent experiments performed in duplicate. The K_i values are calculated using the Cheng and Prusoff equation to correct for the concentration of the radioligand used in the assay. [h] Reference 13. [i] Reference 14. [j] Reference 38.

Table 2. Functional Assay Results for Bifunctional Peptide Derivative Ligands at Opioid and Substance P Receptors

	opioid agonist		substance P antagonist
	MVD (δ)	GPI (μ)	GPI
compd	IC_{50} (nM)[a]	IC_{50} (nM)[a]	K_e (nM)[b]
1[c]	15 ± 2	490 ± 29	10 ± 2
2[d]	14 ± 2	460 ± 160	10 ± 3
3	2.3 ± 0.6	68 ± 10	13 ± 4
4	14 ± 1	110 ± 27	6.1 ± 0.8
5	8.7 ± 2.5	22 ± 2	14 ± 6
6	8.8 ± 2.1	23 ± 3.6	24 ± 2
7	1.8 ± 0.6	19 ± 5	7.5 ± 0.5
Biphalin	2.7 ± 1.5	8.8 ± 0.3	
L-732,138			250 ± 87

[a] Concentration at 50% inhibition of muscle contraction at electrically stimulated isolated tissues (n = 4). [b] Inhibitory activity against the substance P induced muscle contraction in the presence of 1 μM naloxone, K_e: concentration of antagonist needed to inhibit substance P to half its activity (n = 4). [c] Reference 13. [d] Reference 14.

the importance of modification at C-terminus for both μ- and δ- opioid agonist activities. However, the NK1 affinities of **6** were decreased (K_i = 0.95 and 320 nM for human and rat NK1 receptors, respectively).

Finally, we introduced Dmt[1] on compound **1**, which has a Met in the fifth position where the two pharmacophores are connected (**7**, Figure 1). In contrast with compound **3** with a Nle[5] residue, the binding affinity of **7** at the hNK1 receptors was as potent as those of **1** and **2**. Compound **7** also showed potent antagonist activity against substance P stimulation in the GPI tissue in the presence of naloxone. At the opioid receptors, the affinities of **7** were improved from those of **1** and **2**, showing subnanomolar opioid affinities at the DOR and a potent K_i value at the MOR (K_i = 0.18 and 2.0 nM, respectively) (Table 1). The observed high opioid affinities of **7** were maintained in the GTPγS binding assays with highly efficacious EC_{50} and E_{max} values (94 and 72% for DOR and MOR, respectively, Table 3). The opioid activities of **7** also were improved from those of **1** by 8- and 26-fold in the isolated tissue bioassays using the MVD and GPI, respectively (IC_{50} = 1.8 and 19 nM, respectively). These results clearly suggest that Nle, which is generally considered as a bioisostere of Met, does not necessarily produce similar activities as derivatives with Met. It is also demonstrated that the fifth position is important for affinities and activities of δ/μ opioid/NK1 bifunctional peptide derivatives possessing Dmt[1].

Considering all the biological results for the opioid and NK1 receptors, **7** was found to have the most improved bifunctional affinities and activities compared to the lead compounds **1** and **2**.

In Vitro Metabolic Stability. For further biological characterization, the metabolic stability of **7** was tested by incubation in rat plasma at 37 °C.[14] The degradation curve of **7** was significantly improved from that of **1** and was as stable as that of **2**, suggesting that Dmt[1]-introduction (**7**) and Nle[5]-incorporation (**2**) in **1** had a similar positive effect against recognition by degrading enzymes (Figure 2). This improved metabolic stability together with the excellent bifunctional activities motivated us to perform in vivo animal studies using compound **7** to confirm its in vivo analgesic efficacy.

In Vivo Antinociceptive Effect. Acute intrathecal (i.t.) injection of **7** was given to normal rats to investigate its antinociceptive properties. A dose of 10 μg of **7** resulted in paw withdrawal latencies of 28 ± 2.6 s, which is significantly higher when compared to baseline values (23 ± 0.9 s) or vehicle treatment (20 ± 2.2 s) alone ($p < 0.05$; Figure 3). The antinociceptive effect of **7** over baseline at 60 min is 52 ± 22%, whereas vehicle is 7.0 ± 5.7% over baseline following i.t. administration.[23] As reported previously,[21] our preliminary result showed that the observed peak effect of **1** occurred between 15 and 30 min after the i.t. injection using the same animal model; in this study, compound **7** produced maximal antinociception at 60 min when **1** showed no significant efficacy. When compared to i.t. morphine, the time of peak effect for similar doses is different (20 min for morphine and 60 min for **7**) although the efficacy is similar. These results may have relevance to the observed stabilities of **7** in rat plasma, although existing peptidases in the central nervous system may not be the same as those in plasma.

In conclusion, **7** showed excellent bioactivities for both the opioid receptors and the NK1 receptors, effective antinociceptive potential in vivo, and longer half-life than the lead compound **1**.

Table 3. Opioid Agonist Functional Activities in [^{35}S]GTPγS Binding Assays

	hDOR[a]			rMOR[a]		
compd	Log EC_{50}[b]	EC_{50} (nM)[c]	E_{max} (%)[d]	Log EC_{50}[b]	EC_{50} (nM)[c]	E_{max} (%)[d]
1[e]	−8.07 ± 0.11	8.6	60 ± 2	−8.16 ± 0.17	7.0	51 ± 3
2[f]	−8.30 ± 0.09	5.0	120 ± 3	−7.74 ± 0.14	18	66 ± 3
3	−9.90 ± 0.34	0.10	41 ± 7	−9.24 ± 0.14	0.57	46 ± 2
4	−8.15 ± 0.22	2.3	49 ± 2	−8.10 ± 0.19	8.0	29 ± 1
5	−9.36 ± 0.16	0.20	50 ± 3	−9.08 ± 0.28	0.83	17 ± 1
6	−9.24 ± 0.17	0.60	42 ± 2	−9.02 ± 0.15	0.72	48 ± 2
7	−9.01 ± 0.17	1.0	94 ± 4	−7.54 ± 0.27	29	72 ± 4
Biphalin	−8.95 ± 0.17	1.1	83			
DAMGO				−7.44 ± 0.19	37	150

[a] Expressed from HN9.10 cell. [b] The log EC_{50} ± standard error are logarithmic values determined from the nonlinear regression analysis of data collected from at least two independent experiments performed in duplicate. [c] Antilogarithmic value of the respective EC_{50}. [d] [total bound − basal]/[basal − nonspecific] × 100 [e] Reference 13. [f] Reference 14.

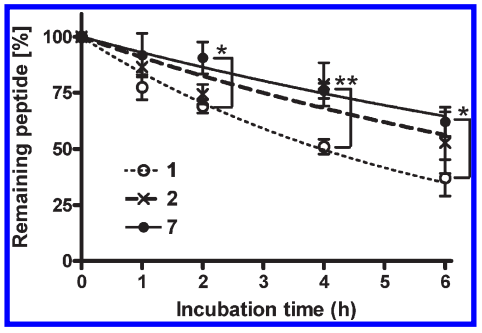

Figure 2. Comparison of the in vitro metabolic stability for **1**[14] (open circle), **2**[14] (crosses), and **7** (filled circle) incubated in rat plasma at 37 °C. Calculated half-lives of peptide derivatives ($T_{1/2}$) were 4.8 h for **1** and >6 h for **2** and **7**. The samples were tested in three independent experiments ($n = 3$), and the mean values were used for the analysis with the SD. Statistical significance was determined by Kruskal−Wallis test followed by Tukey's test. Asterisks denote significant differences (* $p < 0.05$; ** $p < 0.01$).

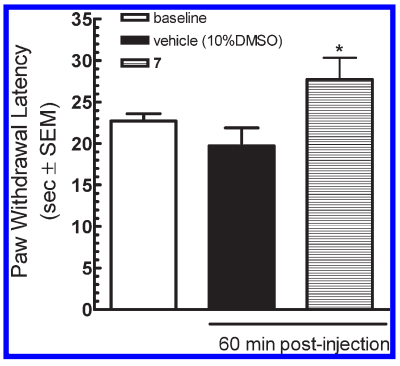

Figure 3. Animals underwent intrathecal cannulation and were allowed 5−7 days recovery. Baseline paw withdrawal latencies were obtained 30 min prior to compound or vehicle administration ($n = 11$) and rats then randomized to a treatment group. **7** (10 μg in 5 μL, $n = 5$) produced maximal antinociception 60 min after the i.t. injection. *$p < 0.05$ compared to both baseline and vehicle ($n = 6$) paw withdrawal latencies.

^{1}H NMR Studies in Membrane-Mimicking Circumstances for Conformational Calculation. To elucidate the biological and conformational effect of Dmt^1-incorporation, we next performed NMR structural analysis of **7**. In fact, numerous SAR studies on

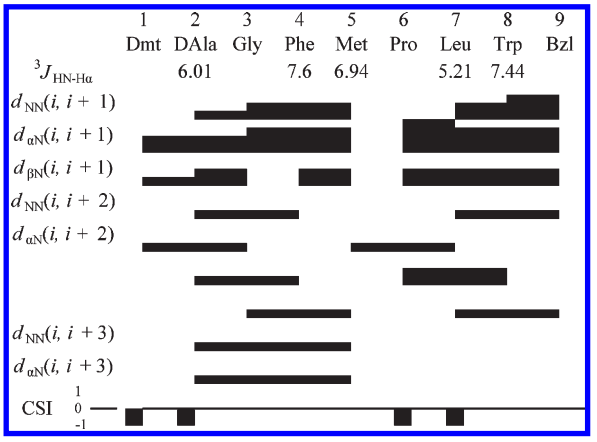

Figure 4. Diagram of H^N-H^α coupling constants, NOE connectivities, and H^α chemical shift index (CSI) for **7**. The H^α CSI was calculated using the random-coil values reported by Andersen et al.[40,42,43] The residue Bzl stands for the respective *C*-terminal moieties.

Dmt^1-enkephalin derivatives have been reported, e.g. 25−27, but little is known about the conformational affect that may result from a Tyr^1-to-Dmt^1 substitution. Thus, the conformation of **7** in membrane-mimicking micelles was compared with the previously obtained NMR structure of **1** using the same conditions and procedures[13] to evaluate any conformational difference.

The two-dimensional ^{1}H NMR studies of **7** including total correlation spectroscopy (TOCSY), double quantum filtered correlation spectroscopy (DQF-COSY), and nuclear Overhauser enhancement spectroscopy (NOESY), were performed in pH 4.5 buffer (45 mM CD_3CO_2Na/HCl, 1 mM NaN_3, 90% H_2O/10% D_2O) with a 40-fold excess of perdeuterated dodecylphosphocholine (DPC) micelles (Figure 4). DPC is a widely used lipid-like surfactant to evaluate the solution NMR structures of membrane-bound proteins and peptides, e.g. 13,28−30. The important relevance of membrane-bound conformations of ligands for GPCRs and their biological activities have been extensively discussed recently, e.g.13,30,31. All ^{1}H chemical shift assignments of **7** are found in the Supporting Information.

Conformational Analysis. The total number of used nuclear Overhauser enhancement (NOE) restraints for structural calculation of **1** was 155, while that of **7** was 169, including 62 intraresidual NOEs, 67 sequential NOEs, 49 medium-range

Table 4. Atomic rmsd Values (Å) for the Final 19 Conformers Compared to the Most Stable Conformer of Bifunctional Peptide Derivatives

	1[a]	7
Backbone Atoms (N, C^{α}, C′)		
calcd on whole molecule	1.14 ± 0.43	0.86 ± 0.21
calcd only on 1−4 residues	1.05 ± 0.63	0.55 ± 0.28
calcd only on 5−8 residues	0.45 ± 0.38	0.19 ± 0.10
All Non-hydrogen Atoms		
calcd on whole molecule	2.09 ± 0.64	1.91 ± 0.54
calcd only on 1−4 residues	2.16 ± 0.98	1.33 ± 1.01
calcd only on 5−8 residues and C-terminus	1.02 ± 0.25	1.27 ± 0.41

[a] Reference 13.

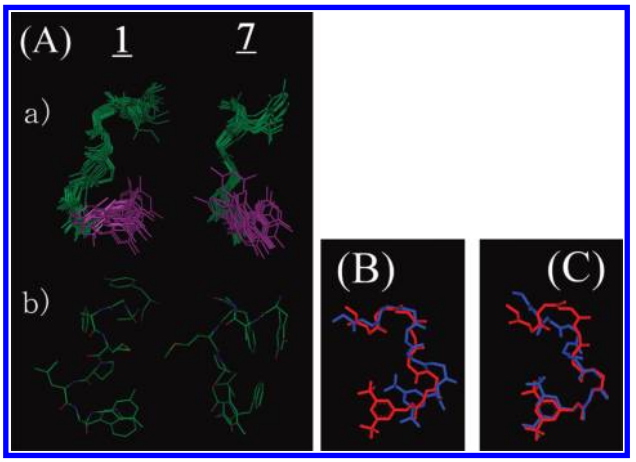

Figure 5. (A) Ensembles of the best 20 calculated structures in 40-fold DPC micelle/pH 4.5 buffer for **1**[13] (left) and **7** (right) with the lowest restraint energy, aligned on backbone atoms of residues (a) 1−8. The aligned structures are illustrated the backbone atoms with C-terminal benzyl moiety (purple). (b) The most stable conformers are shown with all heavy atoms (C, N, O, and F). The superimposed images of obtained NMR structure of **7** (red) with the NMR structure of **1** (blue) at the lowest restraint energy for opioid pharmacophore (residues 1−4 (B)) and for NK1 pharmacophore (residues 6-C-terminus (C)).

NOEs (2−4 residues), and 5 long-range NOEs (>4 residues). The ^{1}H NMR spectra in **7** showed a negligible amount of the minor cis/trans rotamer at the Pro^{6} residue. In the structural calculation, the Met^{5}−Pro^{6} bond of the major rotamer was fixed in the trans configuration based on the observation of Met^{5} H^{α} to Pro^{6} H^{δ} sequential NOEs together with the absence of sequential Met^{5} H^{α}−Pro^{6} H^{α} NOEs. The restrained molecular dynamics calculations[32,331] were performed based on the observed NOE restraints, and the calculated 20 lowest-energy structures from this analysis were used for the structural analysis of **7**. The calculated 20 structures for **7** showed a very small number of violations for total NOE restraints, maximum NOE distances, and restraint energy based on the Amber force field (details are provided in the Supporting Information).

The conformational effect of Dmt^{1}-incorporation in place of Tyr^{1} was observed on the obtained NMR structures of **7** in the presence of membrane-mimicking DPC micelles. The calculated superimposed structures of **7** for the alignments on the entire molecule showed smaller root-mean-square deviation (rmsd)

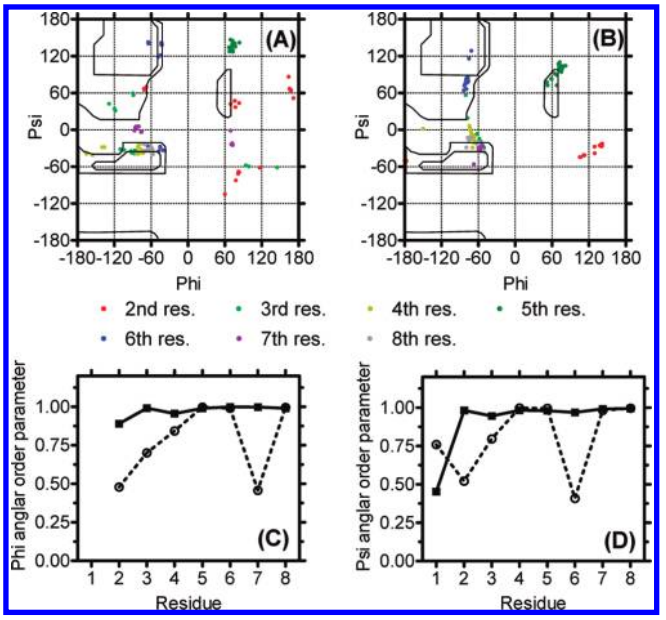

Figure 6. The Ramachandran φ,ψ plots for (A) **1** and (B) **7** for residues 2−7 of 20 final structures. Angular order parameters[32,34] for φ (C) and ψ (D) angles calculated from the 20 final structures for **1**[13] (open circle) and **7** (filled square), respectively. For calculating the ψ angles of Trp^{8}, the nitrogen atoms of C-terminal benzyl amide were used instead of N $(i + 3)$, respectively.

values than those of **1** (0.86 for backbone atoms and 1.91 for all heavy atoms; Table 4 and Figure 5A). Especially, those for the alignment on the residues 1−4 were smaller, indicating that the introduction of Dmt^{1}, possessing two methyl groups on its phenyl ring, provided a more defined N-terminus conformation compared to that of **1** (rmsd = 0.55 for backbone atoms and 1.33 for all heavy atoms). For the C-terminal half of **7**, the structural definition of backbone atoms also were improved, while non-hydrogen atoms were rather poorly defined compared to those of **1** (rmsd = 0.19 for backbone atoms and 1.27 for all heavy atoms).

The better defined conformation of **7** in the N-terminal region compared to **1** was also confirmed based on the analysis using backbone φ and ψ torsion angles. The residues 2 and 3 in the 20 best structures of **1** had rather scattered plots in the Ramachandran diagram, while those in **7** were highly aggregated (Figure 6A,B). The φ and ψ angular order parameters[34] of residues 2 and 3 were close to one in **7**, but not in **1** (Figure 6C,D). The Dmt^{1}-introduction also changed a number of β-turn structural elements in the N-terminus. The NMR structure of **1** had two β-turns at the residues 2−5 and 6 to the C-terminus.[13] These two turn structures also were observed in **7** (Table 5). Additionally, 12 out of 20 of the best structures of **7** showed a distance between the C_{α} of Tyr^{1} and the C_{α} of Phe^{4} within 7 Å, whereas **1** had the same β-turn structural elements only in three structures. Thus, the N-terminus of **7** manifested the better-defined conformation with more definitive β-turns compared to that in **1**.

These results indicate that **7** clearly has a more structured conformation than **1**, especially close to the site of the Dmt^{1}-incorporation, probably due to steric and lipophilic differences between Dmt and Tyr. The introduction of two methyl groups in the first residue plays a crucial role in the molecular structure of opioid pharmacophore, suggesting shifts of affinities and efficacies at the opioid receptors, as observed.

dx.doi.org/10.1021/jm101023r |J. Med. Chem. 2011, 54, 2029–2038

Table 5. Number of β-Turn Structural Elements and the Distance between α Carbons of ith and $(i+3)$rd Residues[a]

	1[b]		7	
residues	number of structures with β-turns	distance (Å)	number of structures with β-turns	distance (Å)
$C^1\alpha-C^4\alpha$	3	7.86 ± 1.21	12	6.85 ± 0.64
$C^2\alpha-C^5\alpha$	20	4.95 ± 0.71	20	5.93 ± 0.35
$C^6\alpha-$Bzl	19	6.32 ± 0.43	20	5.45 ± 0.21

[a] Out of the best 20 calculated structures. The distance is the mean distance between two α carbons ± standard deviation (SD). The sequences with less than 7 Å distance between α carbons of ith and $(i+3)$rd residues without helical structure were considered as a β-turn.[41] Bzl stands for the benzyl moiety at the *C*-terminus. [b] Reference 13.

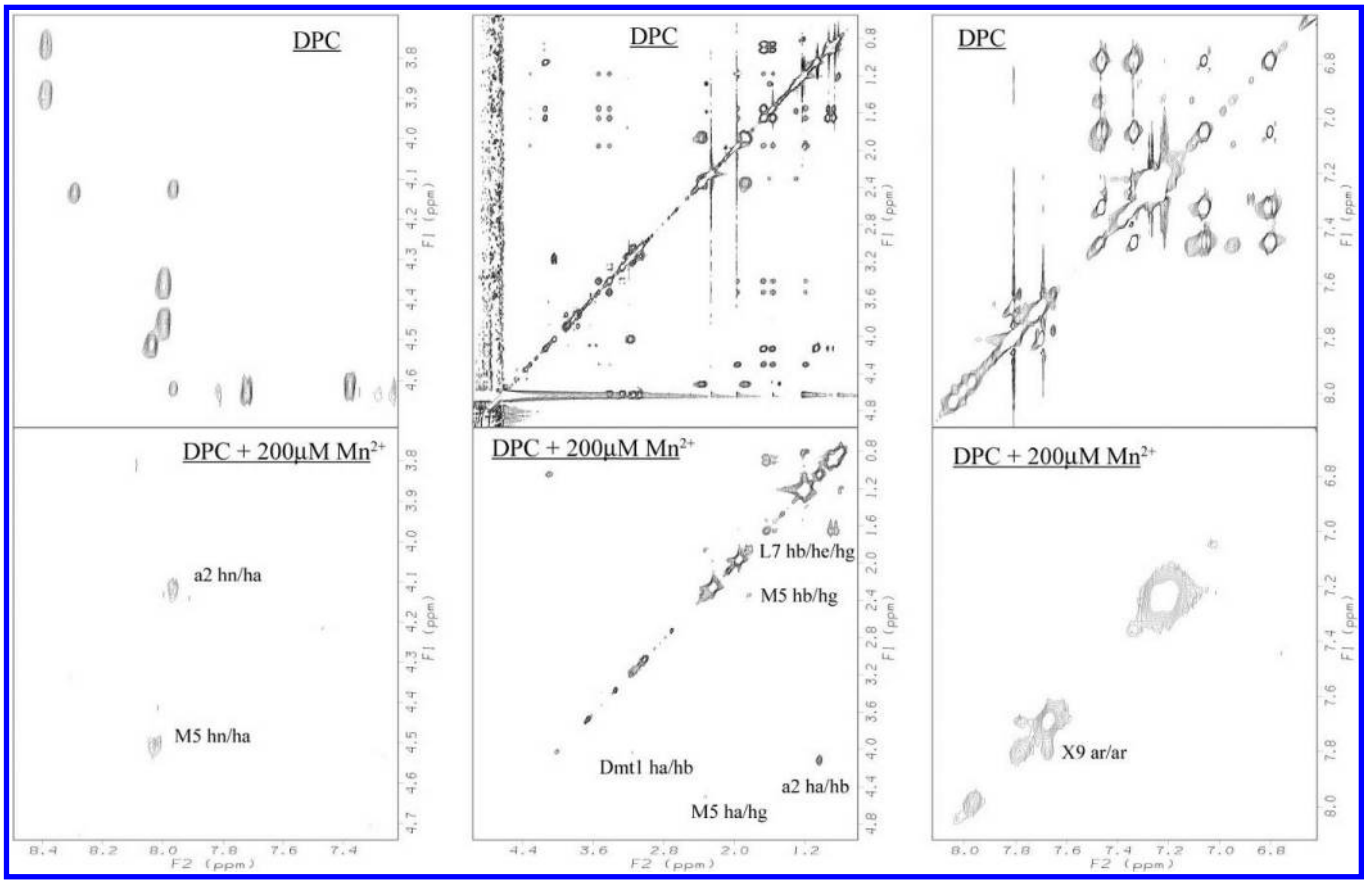

Figure 7. The paramagnetic effects on TOCSY Spectra of **7**. **7** with DPC micelles (top row) and with 200 μM Mn^{2+} (bottom). Preserved resonances (labeled) are in a phase not missed by the phase-specific radical probe (Mn^{2+}). Spectra were compared from the same noise level. X9 represents the cross-peaks derived from the corresponding aromatic protons of benzyl moiety.

The lowest energy structures of **1** and **7** were next superimposed on alignment with the backbone atoms to clarify structural differences due to the Dmt-substitutive effect at the first position. The backbone conformation of the opioid pharmacophore of the two molecules showed similar conformations with good overlap that was further improved when the superimposition was performed for the NK1 pharmacophore which showed nearly complete overlap (Figure 5B). It is interesting to note that when the alignment was made for the opioid pharmacophores of **1** and **7**, the corresponding NK1 pharmacophores was directed differently in 3D space and thus showed almost no overlap. This result indicates that the Tyr^1-to-Dmt^1 substitution changes the relative orientation of two pharmacophores which work as an address region with each other through a conformational change at the fifth residue. The important implication of these results is that the Dmt^1 introduction induces orientational shifts of the C-terminus, and these shifts may lead to additional changes in affinities and efficacies at both opioid and NK1 receptors, depending on the amino acid residue at the fifth residue.

Paramagnetic Broadening Studies on ^{1}H NMR. The interactive mode between the bifunctional compound **7** and the cell membrane was examined in order to investigate the effect of Dmt^1-substitution at the place of Tyr^1 using pseudomembrane conditions. Mn^{2+} was used as a paramagnetic ion to eliminate the resonance intensities of solvent-exposed protons in the DPC micelles based on spin system in TOCSY spectra.[13,16]

Interestingly, two major differences were found for the conformations of **7** and **1**[13] (Figure 7 and Supporting Information). First, a cross-peak of NH and H^α protons in D-Ala^2 was observed

dx.doi.org/10.1021/jm101023r |*J. Med. Chem.* 2011, 54, 2029–2038

for 7but not for **1**, suggesting that the backbone protons in D-Ala^2 of **7** were buried inside of the micelle, while those of **1** were mostly exposed to its surface. This suggests that the Dmt^1-incorporation increased the lipophilicity of the opioid pharmacophore, especially around residue 2, to strengthen peptide−membrane interactions. Second, the aromatic side-chain protons of Trp in **1** were mostly maintained after the Mn^{2+} addition, whereas no corresponding cross-peaks were observed for **7**, suggesting that the side-chain of Trp in **1** is located deeper in the micelle than in **7**. Thus, Dmt^1-incorporation affects the compound−membrane interactions for the side-chains of the C-terminal half, although it is away from the substitution site.

As a result, the Tyr^1-to-Dmt^1 substitution changed backbone conformation of opioid pharmacophore which is modified with an improved β-turn conformation and strengthened interactions between the ligand and membranes. Whereas, the NK1 pharmacophores of **1** and **7** showed similar backbone conformations, the conformation shift was observed primarily in their side chains. Therefore, this substitution has a direct structural effect on the opioid pharmacophore, and changes the orientation of NK1 pharmacophore at the fifth residue with the small conformational shifts in the NK1 pharmacophore. These structural shifts due to the Tyr^1-to-Dmt^1 substitution may have a strong relationship with the ligand-GPCR docking process assisted by cell membrane to critically modulate the affinity and activity of the ligand.

CONCLUSION

In the search for a drug candidate as a novel type of analgesic, optimization on the C-terminus and fifth residue of lead compounds **1** and **2** were performed. Among the synthesized derivatives, **7**, possessing a Dmt^1, a Met^5, and NH-[3′,5′-$(CF_3)_2$-Bzl] at the C-terminus, was found to have improved opioid agonist activities while maintaining NK1 antagonist activity. On the basis of the NMR structural analysis in a membrane-mimicking environment, lipophilic and steric effects of a Dmt^1-residue induce changes in the conformation and in the membrane−ligand interactive mode, not only in the opioid pharmacophore region, but also in the NK1 pharmacophore region which is some distance from the substitution site. The important finding from these results is that the two pharmacophores do not work independently, but concertedly, and their conformational "balance" has a crucial effect on their biological behaviors. Moreover, **7** showed significant antinociceptive activity in vivo and more than 6 h half-life in rat plasma. These results indicate that compound **7** could be considered as a valuable research tool to develop a novel analgesic drug. Further investigations on **7** are presently underway in our laboratory for further in vivo biological characterization.

EXPERIMENTAL SECTION

Materials. All amino acid derivatives, coupling reagents, and resins were purchased from EMD Biosciences (Madison, WI), Bachem (Torrance, CA), SynPep (Dublin, CA), and Chem Impex International (Wood Dale, IL). Perdeuterated DPC was purchased from C/D/N Isotopes (Quebec, Canada). ACS grade organic solvents were purchased from VWR Scientific (West Chester, PA), and other reagents were obtained from Sigma-Aldrich (St. Louis, MO) and used as obtained. Myo-[2-^{3}H(N)]-inositol, [tyrosyl-3,5-^{3}H(N)] D-Ala^2-Mephe^4-glyol^5-enkephalin ([^{3}H]-DAMGO), [tyrosyl-2,6-^{3}H(N)]-(2-D-penicillamine, 5-D-penicillamine)enkephalin ([^{3}H]-DPDPE), [^{3}H]-substance P, and [^{35}S]-GTPγS were purchased from Perkin-Elmer (Wellesley, MA). Bovine serum albumin (BSA), protease inhibitors, Tris, and other buffer reagents were obtained from Sigma (St. Louis, MO). Culture medium, penicillin/streptomycin, and fetal calf serum (FCS) were purchased from Invitrogen (Carlsbad, CA).

Preparation and Characterization of Peptides. The peptides were prepared and purified using the same method as described previously.[9,13,15] All the obtained final peptides showed >98% purity. The purified peptides were characterized by high-resolution mass spectroscopy, TLC, analytical HPLC, and ^{1}H NMR (Supporting Information). Sequential assignment of proton resonances was achieved by 2D-TOCSY NMR experiments.[35] High-resolution MS were taken in the positive ion mode using FAB methods at the University of Arizona Mass Spectrometry Facility. TLC was performed on aluminum sheets coated with a 0.2 mm layer of silica gel 60 F_{254} Merck using the following solvent systems: (1) $CHCl_3$:MeOH:AcOH = 90:10:3, (2) EtOAc:*n*-BuOH:water:AcOH = 5:3:1:1, and (3) *n*-BuOH:water:AcOH = 4:1:1. TLC chromatograms were visualized by UV light and by ninhydrin spray followed by heating (hot plate). Analytical HPLC was performed on a Hewlett-Packard 1100 or Hewlett-Packard 1090m with Waters NOVA-Pak C-18 column (3.9 mm × 150 mm, 5 μm, 60 Å) or Vydac 218TP104 C-18 column (4.6 mm × 250 mm, 10 μm, 300 Å). ^{1}H-1D-NMR spectra were obtained on Bruker DRX-500 or DRX-600 spectrometer. 2D-TOCSY and 2D-NOESY NMR spectra were performed on a Bruker DRX-600 spectrometer equipped with a 5 mm Nalorac triple-resonance single-axis gradient probe. The NMR experiments were conducted in DMSO-d_6 solution at 298 K. Spectra were referenced to residual solvent protons as 2.49 ppm. The processing of NMR data was performed with the XwinNmr software (Bruker BioSpin, Fremont, CA). In the TOCSY experiments, the TPPI mode[36] with MLEV-17 mixing sequence[37] were used with a mixing time of 62.2 ms, at a spin-lock field of 8.33 kHz. The mixing time for the NOESY spectra was 450 ms for all peptide derivatives. All 2D spectra were acquired in the TPPI mode with 2k complex data points in t_2 and 750 real data points in t_1 and the spectral processing using shifted sine bell window functions in both dimensions.

In Vitro Stability of Peptide Derivatives in Rat Plasma.[14,16] Stock solutions of the compound (50 mg/mL in DMSO) were diluted 1000-fold into rat plasma (Lot 24927, Pel-Freez Biologicals, Rogers, AK) to give an incubation concentration of 50 μg/mL of each peptide. All samples were incubated at 37 °C and 200 μL of aliquots were withdrawn at 1, 2, 4, and 6 h. Then 300 μL of acetonitrile was added and the proteins were removed by centrifugation. The supernatant was analyzed for the amount of remaining parent compound by HPLC (Hewlett-Packard 1090m with Vydac 218TP104 C-18 column; 4.6 mm × 250 mm, 10 μm, 300 Å). The samples were tested in three independent experiments (n = 3), and the mean values were used for the analysis with SD.

NMR Spectroscopy in DPC Amphipathic Media and Conformational Structure Determination. All the conformational determinations were performed by the same methods as previously described[13,28,29] based on the NMR spectra using a Bruker DRX600 600 MHz spectrometer.

Briefly, the samples were prepared by dissolving the peptide (3.5 mM) in 0.5 mL of 45 mM sodium acetate-d_3 buffer (pH 4.5) containing 40 equiv of DPC-d_{38} and 1 mM sodium azide (90% H_2O/10% D_2O), followed by sonication for 5 min. DQF-COSY, NOESY[38] (mixing time = 450 ms) and TOCSY spectra[35] (MLEV-17 mixing time = 62.2 ms, spin-lock field = 8.33 kHz) were acquired using standard pulse sequences at 310 K. Coupling constants ($^3J_{NH\text{-}H\alpha}$) were measured from 2D DQF-COSY spectra by analysis of the fingerprint region with a curve-fitting using 5-parameter Levenberg−Marquardt nonlinear least-squares protocol to a general antiphase doublet.

For conformational structure determination, the volumes of the assigned cross-peaks in the 2D NOESY spectrum were converted into upper distance bounds of 3.0, 3.8, 4.8, or 5.8 Å. In addition to the distance constraints, φ dihedral angle constraints derived from $^3J_{HN\text{-}H\alpha}$

coupling constants were set to between −90 and 40° for $^3J_{HN\text{-}H\alpha} < 6$ Hz and to between −150 and −90° for $^3J_{HN\text{-}H\alpha} > 8$ Hz. Dihedral angle constraints of 180 ± 5° for peptide bonds (ω) also were used to maintain the planarity of these bonds. Simulated annealing molecular dynamics analysis was done for all the peptides to obtain an ensemble of NMR structures using NOE-derived distance constraints and dihedral angle (φ) constraints and using the DGII[39] program within the software package Insight II 2000 (Accelrys Inc., San Diego, CA). The final 20 conformations with the lowest energies were used for the analysis. All calculations were performed on a Silicon Graphics Octane computer.

Radioligand Labeled Binding Assay, [^{35}S]GTP-γ-S Binding Assay, GPI, and MVD in Vitro Bioassay. The methods were carried out as previously described.[9,13,15] Briefly, the evaluation of the binding affinities of the synthesized bifunctional peptide derivatives at the human δ-opioid receptors (hDOR) and rat μ-opioid receptors (rMOR) were performed on cell (HN9.10) membranes from cells that stably express the corresponding receptors using [^{3}H]-c[D-Pen^2, D-Pen^5]-enkephalin ([^{3}H]DPDPE) and [^{3}H]-[D-Ala^2, NMePhe^4, Gly^5-ol]-enkephalin ([^{3}H]DAMGO) as the radioligands, for the δ and μ opioid receptors, respectively. Receptor density of the opioid cell lines is generally about 1 pmol/mg of membrane proteins. [^{35}S]GTPγS binding assays were used to examine the δ and μ opioid agonist efficacies on the same cell membranes. Isolated tissue-based functional assays also were used to evaluate opioid agonist activities in the GPI (δ) and MVD (μ). For the affinity at the human NK1 (hNK1) receptors, binding assays utilized membranes from transfected CHO cells that stably express hNK1 receptors, using [^{3}H]-substance P as the standard radioligand. The binding affinity assays at the rat NK1 (rNK1) receptors also were performed using transfected CHO cells that stably express rNK1 receptors. For the human and rat NK1 cell lines, the expressions are about 0.5 and 6 pmol/mg protein, respectively. To evaluate antagonistic activities against substance P stimulation, isolated tissue bioassays using GPI were performed in the presence of naloxone to block the opioid activities.

Experimental Procedure: Determination of Antinociceptive Activities in Vivo of Bifunctional Peptide 7. Male Sprague−Dawley rats (200−225 g; Harlan; Harlan, IN, USA) were obtained and cared for under the University of Arizona IACUC standards. Food and water were available ad libitum. All preparations and testing were performed in accordance with the policies and recommendations of the International Association for the Study of Pain, National Institute of Health and Animal Care, at the University of Arizona. *Intrathecal catheter implantation*: Rats were anesthetized using ketamine/xylazine (vol/vol: 80/20; 100 mg/kg ip) and placed in a stereotaxic head holder. The cisternum magnum was exposed, and an 8 mm catheter was implanted, as described,[40] terminating in the lumbar region of the spinal cord. Animals were allowed to recover for 5−7 days. *Compound administration*: 5 μL of each treatment was given followed 1 μL air bubble/9 μL saline flush over 30 s. *Infrared thermal testing (IR, behavioral)*: Rats were allowed to acclimate within Plexiglas holders for baseline testing (precompound administration) for 20 min. A mobile radiant heat source was used to direct heat to the left hind paw. Paw withdrawal latencies were measured in seconds, with an automatic shutoff of the heat source at 33.0 s. On test days, animals were administered a treatment and tested with radiant heat, 60 min after said administration. Paw withdrawal latencies were calculated and expressed as the mean withdrawal latency ± SEM by Graph Pad Prism 4 (GraphPad Software, La Jolla, CA). One-way analysis of variance (ANOVA) was performed in FlashCalc (University of Arizona, Dr. Michael Ossipov) and statistical significance achieved when $p \leq 0.05$.

■ ASSOCIATED CONTENT

Ⓢ Supporting Information. HR-MS, TLC, HPLC, and ^{1}H NMR data of the peptides **3**−**7** and the metabolic stability studies of peptides **3** in rat plasma are provided. This material is available free of charge via the Internet at http://pubs.acs.org.

■ AUTHOR INFORMATION

Corresponding Author

*Phone: (520)-621-6332. Fax: (520)-621-8407. E-mail: hruby@email.arizona.edu.

Present Addresses

[§]Exploratory Research Laboratories, Ajinomoto Pharmaceuticals Co. Ltd., 1-1 Suzuki-cho, Kawasaki-ku, Kawasaki-shi 210-8681, Japan. E-mail: takashia_yamamoto@ajinomoto.com.

■ ACKNOWLEDGMENT

The work was supported by grants from the USDHS, National Institute on Drug Abuse, DA-13449 and DA-06284. We thank Dr. Guangxin Lin for kind assistance and advice with the NMR measurements, Dr. Eva Varga and Dr. Edita Navratilova for scientific discussion, Magdalena Kaczmarska for culturing cells, and the University of Arizona Mass Spectrometry Facility for the mass spectra measurements. We express appreciation to Margie Colie for assistance with the manuscript.

■ ABBREVIATIONS USED

BSA, bovine serum albumin; CHO, Chinese hamster ovary; DAMGO, [D-Ala^2, NMePhe^4, Gly^5-ol]-enkephalin; Dmt, 2′,6′-dimethyl-L-tyrosine; DOR, δ opioid receptor; DPC, dodecylphosphocholine; DPDPE, c[D-Pen^2, D-Pen^5]-enkephalin; ; DQF-COSY, double quantum filtered correlation spectroscopy; GPI, guinea pig ileum;; GTPγS, guanosine 5′-(γ-thio) triphosphate; i.t., intrathecal; MOR, μ opioid receptor; MVD, mouse vas deferens; NK1, neurokinin 1; NOE, nuclear Overhauser enhancement; NOESY, nuclear Overhauser enhancement spectroscopy; rmsd, root-mean-square deviation; TOCSY, total correlation spectroscopy

■ ADDITIONAL NOTE

Abbreviations used for amino acids and designation of peptides follow the rules of the IUPAC-IUB Commission of Biochemical Nomenclature in *J. Biol.Chem.* **1972**, *247*, 977−983.

■ REFERENCES

(1) Mantyh, P. W.; Allen, C. J.; Ghilardi, J. R.; Rogers, S. D.; Mantyh, C. R.; Liu, H.; Basbaum, A. I.; Vigna, S. R.; Maggio, J. E. Rapid endocytosis of a G protein-coupled receptor: substance P evoked internalization of its receptor in the rat striatum in vivo. *Proc. Natl. Acad. Sci. U.S.A.* **1995**, *92*, 2622–2626.

(2) Kalso, E. Improving opioid effectiveness: from ideas to evidence. *Eur. J. Pain (Amsterdam, Neth.)* **2005**, *9*, 131–135.

(3) King, T.; Ossipov, M. H.; Vanderah, T. W.; Porreca, F.; Lai, J. Is paradoxical pain induced by sustained opioid exposure an underlying mechanism of opioid antinociceptive tolerance?. *Neurosignals* **2005**, *14*, 194–205.

(4) Misterek, K.; Maszczynska, I.; Dorociak, A.; Gumulka, S. W.; Carr, D. B.; Szyfelbein, S. K.; Lipkowski, A. W. Spinal co-administration of peptide substance P antagonist increases antinociceptive effect of the opioid peptide biphalin. *Life Sci.* **1994**, *54*, 939–944.

(5) Powell, K. J.; Quirion, R.; Jhamandas, K. Inhibition of neurokinin-1-substance P receptor and prostanoid activity prevents and reverses the development of morphine tolerance in vivo and the morphine-

induced increase in CGRP expression in cultured dorsal root ganglion neurons. *Eur. J. Neurosci.* **2003**, *18*, 1572–1583.

(6) Ripley, T. L.; Gadd, C. A.; De Felipe, C.; Hunt, S. P.; Stephens, D. N. Lack of self-administration and behavioural sensitisation to morphine, but not cocaine, in mice lacking NK1 receptors. *Neuropharmacology* **2002**, *43*, 1258–1268.

(7) Hruby, V. J. Organic chemistry and biology: chemical biology through the eyes of collaboration. *J. Org. Chem.* **2009**, *74*, 9245–9264.

(8) Horan, P. J.; Mattia, A.; Bilsky, E. J.; Weber, S.; Davis, T. P.; Yamamura, H. I.; Malatynska, E.; Appleyard, S. M.; Slaninova, J.; Misicka, A.; Lipowski, A. W.; Hruby, V. J.; Porreca, F. Antinociceptive Profile of Biphalin, a Dimeric Enkephalin Analog. *J. Pharmacol. Exp. Ther.* **1993**, *265*, 1446–1454.

(9) Yamamoto, T.; Nair, P.; Davis, P.; Ma, S. W.; Navratilova, E.; Moye, M.; Tumati, S.; Vanderah, T. W.; Lai, J.; Porreca, F.; Yamamura, H. I.; Hruby, V. J. Design, Synthesis and Biological Evaluation of Novel Bifunctional C-terminal Modified Peptides for δ/μ Opioid Receptor Agonists and Neurokinin-1 Receptor Antagonists. *J. Med. Chem.* **2007**, *50*, 2779–2786.

(10) Cascieri, M. A.; Macleod, A. M.; Underwood, D.; Shiao, L. L.; Ber, E.; Sadowski, S.; Yu, H.; Merchant, K. J.; Swain, C. J.; Strader, C. D.; Fong, T. M. Characterization of the interaction of *N*-acyl-L-tryptophan benzyl ester neurokinin antagonists with the human neurokinin-1 receptor. *J. Biol. Chem.* **1994**, *269*, 6587–6591.

(11) MacLeod, A. M.; Merchant, K. J.; Cascieri, M. A.; Sadowski, S.; Ber, E.; Swain, C. J.; Baker, R. *N*-Acyl-L-tryptophan benzyl esters: potent substance P receptor antagonists. *J. Med. Chem.* **1993**, *36*, 2044–2045.

(12) Millet, R.; Goossens, L.; Goossens, J. F.; Chavatte, P.; Bertrand-Caumont, K.; Houssin, R.; Henichart, J. P. Conformation of the tripeptide Cbz-Pro-Leu-Trp-OBzl(CF3)2 deduced from two-dimensional ^{1}H NMR and conformational energy calculations is related to its affinity for NK1-receptor. *J. Pept. Sci.* **2001**, *7*, 323–330.

(13) Yamamoto, T.; Nair, P.; Jacobsen, N. E.; Davis, P.; Ma, S. W.; Navratilova, E.; Lai, J.; Yamamura, H. I.; Vanderah, T. W.; Porreca, F.; Hruby, V. J. The Importance of Micelle-Bound States for the Bioactivities of Bifunctional Peptide Derivatives for δ/μ Opioid Receptor Agonists and Neurokinin 1 Receptor Antagonists. *J. Med. Chem.* **2008**, *51*, 6334–6347.

(14) Yamamoto, T.; Nair, P.; Jacobsen, N. E.; Vagner, J.; Kulkarni, V.; Davis, P.; Ma, S.-W.; Navratilova, E.; Yamamura, H. I.; Vanderah, T. W.; Porreca, F.; Lai, J.; Hruby, V. J. Improving metabolic stability by glycosylation: bifunctional peptide derivatives that are opioid receptor agonists and neurokinin 1 receptor antagonists. *J. Med. Chem.* **2009**, *52*, 5164–5175.

(15) Yamamoto, T.; Nair, P.; Vagner, J.; Davis, P.; Ma, S. W.; Navratilova, E.; Moye, M.; Tumati, S.; Vanderah, T. W.; Lai, J.; Porreca, F.; Yamamura, H. I.; Hruby, V. J. A Structure−Activity Relationship Study and Combinatorial Synthetic Approach of C-Terminal Modified Bifunctional Peptides That Are δ/μ Opioid Receptor Agonists and Neurokinin 1 Receptor Antagonists. *J. Med. Chem.* **2008**, *51*, 1369–1376.

(16) Yamamoto, T.; Nair, P.; Davis, P.; Ma, S.-W.; Yamamura, H. I.; Vanderah, T. W.; Porreca, F.; Lai, J.; Hruby, V. J. The biological activity and metabolic stability of peptidic bifunctional compounds that are opioid receptor agonists and neurokinin 1 receptor antagonists with a cystine moiety. *Bioorg. Med. Chem.* **2009**, *17*, 7337–7343.

(17) Hokfelt, T.; Kellereth, J. O.; Nilsson, G. Immunohistochemical studies on the localization and distribution of substance P in cat primary sensory neurons. *Brain Res.* **1975**, *100*, 235–252.

(18) Marchand, J. E.; Kream, R. M. Substance P and Somatostatin levels in rhumatioid arthesis, molecular physiology. In *Substance P and Related Peptides: Cellular and Molecular Physiology*; New York Academy of Science: New York, 1990; pp 437−438.

(19) Kondo, I.; Marvizon, J. C.; Song, B.; Salgado, F.; Codeluppi, S.; Hua, X. Y.; Yaksh, T. L. Inhibition by spinal mu- and delta-opioid agonists of afferent-evoked substance P release. *J. Neurosci.* **2005**, *25*, 3651–3660.

(20) Largent-Milnes, T. M.; Yamamoto, T.; Davis, P.; Ma, S. W.; Hruby, V. J.; Yamamura, H. I.; Lai, J.; Porreca, F.; Vanderah, T. W. Dual acting opioid agonist/NK1 antagonist reverses neuropathic pain and does not produce tolerance. Society for Neuroscience, San Diego, CA, 2007, Poster 725. Visceral Pain: Transmitters and Receptors.

(21) Largent-Milnes, T. M.; Yamamoto, T.; Nair, P.; Navratrilova, E.; Davis, P.; Ma, S.-W.; Hruby, V. J.; Yamamura, H. I.; Lai, J.; Porreca, F.; Vanderah, T. W. Dual acting opioid agonist/NK1 antagonist peptide reverses neuropathic pain in an animal model without demonstrating common opioid unwanted side effects. International Association for the Study of Pain/12th World Congress on Pain, Glasgow, Scotland, 2008.

(22) Largent-Milnes, T. M.; Yamamoto, T.; Campos, C. R.; Corral-Frias, N. S.; Andrade-Jimenez, J. M.; Davis, P.; Ma, S. W.; Mantyh, P. W.; French, E. D.; Davis, T. P.; Lai, J.; Hruby, V. J.; Porreca, F.; Vanderah, T. W. Dual acting opioid agonist/NK1 antagonist does not produce antinociceptive tolerance or reward in an animal model of neuropathic pain. Society for Neuroscience, Chicago, IL, 2009, Program/Poster: 255.10/U7.

(23) Largent-Milnes, T. M.; Yamamoto, T.; Nair, P.; Hruby, V. J.; Yamamura, H. I.; Lai, J.; Porreca, F.; Vanderah, T. W. Spinal or systemic TY005, a peptidic opioid agonist/neurokinin 1 antagonist, attenuates pain with reduced tolerance. *Br. J. Pharmacol.* **2010**, *161*, 986–1001.

(24) Bryant, S. D.; Jinsmaa, Y.; Salvadori, S.; Okada, Y.; Lazarus, L. H. Dmt and opioid peptides: a potent alliance. *Biopolymers* **2003**, *71*, 86–102.

(25) Lee, Y. S.; Petrov, R.; Park, C. K.; Ma, S. W.; Davis, P.; Lai, J.; Porreca, F.; Vardanyan, R.; Hruby, V. J. Development of novel enkephalin analogues that have enhanced opioid activities at both mu and delta opioid receptors. *J. Med. Chem.* **2007**, *50*, 5528–5532.

(26) Sasaki, Y.; Suto, T.; Ambo, A.; Ouchi, H.; Yamamoto, Y. Biological properties of opioid peptides replacing Tyr at position 1 by 2,6-dimethyl-Tyr. *Chem. Pharm. Bull.* **1999**, *47*, 1506–1509.

(27) Hansen, D. W., Jr.; Stapelfeld, A.; Savage, M. A.; Reichman, M.; Hammond, D. L.; Haaseth, R. C.; Mosberg, H. I. Systemic analgesic activity and delta-opioid selectivity in [2,6-dimethyl-Tyr1,D-Pen2,D-Pen5]enkephalin. *J. Med. Chem.* **1992**, *35*, 684–687.

(28) Jacobsen, N. E.; Abadi, N.; Sliwkowski, M. X.; Reilly, D.; Skelton, N. J.; Fairbrother, W. J. High-resolution solution structure of the EGF-like domain of heregulin-alpha. *Biochemistry* **1996**, *35*, 3402–3417.

(29) Ying, J.; Ahn, J. M.; Jacobsen, N. E.; Brown, M. F.; Hruby, V. J. NMR solution structure of the glucagon antagonist [desHis1, desPhe6, Glu9]glucagon amide in the presence of perdeuterated dodecylphosphocholine micelles. *Biochemistry* **2003**, *42*, 2825–2835.

(30) D'Alagni, M.; Delfini, M.; Di Nola, A.; Eisenberg, M.; Paci, M.; Roda, L. G.; Veglia, G. Conformational study of [Met5]enkephalin-Arg-Phe in the presence of phosphatidylserine vesicles. *Eur. J. Biochem.* **1996**, *240*, 540–549.

(31) Deber, C. M.; Behnam, B. A. Role of membrane lipids in peptide hormone function: binding of enkephalins to micelles. *Proc. Natl. Acad. Sci. U.S.A.* **1984**, *81*, 61–65.

(32) Weiner, S. J.; Kollman, P. A.; Case, D. A. An all atom force field for simulations of proteins and nucleic acids. *J. Comput. Chem.* **1986**, *7*, 230–252.

(33) Weiner, S. J.; Kollman, P. A.; Case, D. A.; Singh, U. C.; Ghio, C.; Alagona, G. S.; Profeta, J.; Weiner, P. A New Force Field for Molecular Mechanical Simulation of Nucleic Acids and Proteins. *J. Am. Chem. Soc.* **1984**, *106*, 765–784.

(34) Hyberts, S. G.; Goldberg, M. S.; Havel, T. F.; Wagner, G. The solution structure of eglin c based on measurements of many NOEs and coupling constants and its comparison with X-ray structures. *Protein Sci.* **1992**, *1*, 736–751.

(35) Davis, D. G.; Bax, A. Assignment of complex proton NMR spectra via two-dimensional homonuclear Hartmann−Hahn spectroscopy. *J. Am. Chem. Soc.* **1985**, *107*, 2820–2821.

(36) Marion, D. W., K. Application of phase sensitive two-dimensional correlated spectroscopy (COSY) for measurements of 1H−1H spin-spin coupling constants in proteins. *Biochem. Biophys. Res. Commun.* **1983**, *113*, 967–974.

(37) Braunschweiler, L.; Ernst, R. R. Coherence Transfer by Isotropic Mixing: Application of Proton Correlation Spectroscopy. *J. Magn. Reson.* **1983**, *53*, 521–528.

(38) Kumar, A.; Ernst, R. R.; Wüthrich, K. A two-dimensional nuclear Overhauser enhancement (2D NOE) experiment for the elucidation of complete proton−proton cross-relaxation networks in biological macromolecules. *Biochem. Biophys. Res. Commun.* **1980**, *95*, 1–6.

(39) Havel, T. F. An evaluation of computational strategies for use in the determination of protein structure from distance constraints obtained by nuclear magnetic resonance. *Prog. Biophys. Mol. Biol.* **1991**, *56*, 43–78.

(40) Yaksh, T. L.; Rudy, T. A. Chronic catheterization of the spinal subarachnoid space. *Physiol. Behav.* **1976**, *17*, 1031–1036.

(41) Wagner, G.; Neuhaus, D.; Worgotter, E.; Vasak, M.; Kagi, J. H.; Wuthrich, K. Nuclear magnetic resonance identification of "half-turn" and 3(10)-helix secondary structure in rabbit liver metallothionein-2. *J. Mol. Biol.* **1986**, *187*, 131–135.

(42) Wishart, D. S.; Sykes, B. D.; Richards, F. M. The Chemical Shift Index: A Fast and Simple Method for the Assignment of Protein Secondary Structure through NMR Spectroscopy. *Biochemistry* **1992**, *31*, 1647–1651.

(43) Andersen, N. H.; Neidigh, J. W.; Harris, S. W.; Lee, G. M.; Liu, Z. H.; Tong, H. Extracting Information from the Temperature Gradients of Polypeptide NH Chemical Shifts. 1. The Importance of Conformational Averaging. *J. Am. Chem. Soc.* **1997**, *119*, 8547–8561.